CHALMERS

A method to compartmentalize a high shear granulator

Master of Science Thesis in the Master Degree Program:
Innovative and Sustainable Chemical Engineering

PATRIC KVIST

Department of Chemical and Biological Engineering
CHALMERS UNIVERSITY OF TECHNOLOGY
Gothenburg, Sweden 2014

A method to compartmentalize a high shear granulator

Master of Science Thesis in the Master Degree Program: Innovative and Sustainable Chemical Engineering

PATRIC KVIST

Department of Chemical and Biological Engineering
Chalmers University of Technology
SE-412 96 Göteborg
Sweden
Telephone + 46 (0)31-772 1000

Abstract

High shear granulation is a process that is present in a large variety of fields, such as pharmaceutical, specialty chemicals, detergents and many more. The process consists of three main steps; dry mixing, liquid addition and wet massing after which granules of desired properties are produced. Key properties of granules include size and strength.

Modeling of the granulation process is normally done with population balances where the population of granules is tracked over time. To track the size of the granules different mechanisms can be modeled such as growth, breakage and nucleation.

Computational simulations of the flow field are performed to understand how particle interactions occur in the system and are often done in the lagrangian framework. Even though this gives detailed information of the system it is not a feasible approach for large scale units. Instead continuum modeling is applied where particles are regarded as a continuous phase.

The aim of this thesis is to develop a method to utilize compartment modeling as a way to integrate continuum modeling with population balance modeling. A hybrid model has the advantage of not being as computationally heavy as augmenting the flow field simulations with additional population balance equations, but still have information from the flow field incorporated in the model. Another advantage is that non ideal mixing can be simulated for an entire unit by separating gradients in the system into different compartments.

Different methods to compartmentalize the granulator based on CFD simulations in Fluent 13 with user defined functions are evaluated. A method that makes use of a cell looping macro is found to be very efficient and accurate for creating compartments.

Results indicate that high shear granulation is a well-mixed process with regards to aggregation kernels and that the limiting factor appears to be the high flow rates of particles.

Keywords: High shear granulation, compartment modeling, CFD, continuum modeling.

Acknowledgements

I would like to thank my supervisor Per Abrahamsson who has helped me during the whole thesis and made it a very enjoyable time.

Examiner Professor Ander Rasmuson for having me here at the department.

Gavin Reynolds and Ingela Niklasson Björn for supplying and giving support on the use of the PBM code, and good discussions.

Xi Lu for his previous work on the user defined functions in Fluent.

The whole department of chemical engineering for a great time.

My fellow thesis workers.

Table of Contents

1. Introduction

High shear granulation is a process in which granules are created from powder by addition of a liquid binder and impeller agitation. Granulation is applied in several different industries, including pharmaceuticals, mineral processing, specialty chemicals and foodstuffs and in the chemical industry alone annual value of particulate and powder products estimate over 1 trillion US$ [1]. Even though high shear granulation is a process that is widely used it is still practiced more as an art rather than a science with significant failures during scale-up and difficulties predicting both size and properties of granules [1], [2].

Three key steps can be seen in this process; first is the dry mixing step where the dry ingredients are mixed until homogenous. These particles are often called primary particles or fines. After the mixing stage is done, liquid binder is added to the system through a spray nozzle. To disperse the binder as thoroughly as possible a fine spray with small droplets is preferred. The wet mix is then worked for a certain time until granules of desired properties and size is reached in what is called the wet massing stage.

With the development of more powerful computers and efficient commercial programs computational fluid dynamics (CFD) has been used to model the flow field of granulators. Simulations of the flow field are often restricted to one specific stage of the granulation process since augmenting the simulations with population balance equations to track the whole granulation process is simply to computationally heavy [3].

Two main approaches to model the flow field are either a discrete element (DEM) approach where individual particles are tracked or a continuum approach. Tracking individual particles are computationally heavy and more or less impossible to use when scale-up is of interest in particulate systems. In the continuum approach, particles are considered as a continuous phase. This includes a loss of individuality for particles but has an advantage of being easier to scale-up. Darelius et al [4] and Ng et al [5] were the first to use a continuum approach to granulation. This has further been studied by Abrahamsson et al [6] and developed by Mohammed et al [7] which shows promising results but also a need for further development.

To describe the evolution of properties throughout the granulation process, such as granule size distribution, population balance modeling (PBM) is often applied. Rate of change of properties are described by so-called kernels that contain mechanisms present in the system. The main mechanisms that influence size distribution include wetting and nucleation, consolidation and growth, attrition and breakage [1], [8]. Tan et al [9] has demonstrated how a growth kernel can be derived based on the kinetic theory of granular flow to include random particle motion as a time dependent part next to the more classical size dependent aggregation kernel developed by Hounslow. Darelius et al [10] compared different coalescence kernels to experimental results and Nilpawar et al [2] has examined aggregation efficiency by experimentally observing surface velocity fluctuations to estimate collision frequency.

The aim of this thesis is to develop a method that can compartmentalize a granulator volume based on CFD information to aid in the connection between macro-scale PBM and meso-scale CFD flow field modeling to achieve a multi-scale model that can utilize information from both models in conjunction with each other. To achieve this, a compartmental modeling approach is suggested in which the granulator volume is divided into smaller volumes, called compartments, which are connected to each other by flow rates to and from the compartments. Each compartment contains a population balance equation consisting of granulation mechanisms. The connective flow rates between the compartments will allow the population balance to have spatial variations. Traditionally it has been quite hard to estimate fluxes between boundaries, or determine them experimentally when applying compartmental modeling [3]. However with the aid of CFD simulations this type of modeling can be done more freely.

A theoretical framework [3], as well as an automatic zoning process [11] for hybrid compartmental-CFD modeling were developed by Bezzo et al. Bezzo later applied this framework to a batch bioreactor [12] to account for imperfect mixing with regard to viscosity. Another approach by Iliuta et al [13] using compartments to separate gasification and combustion to solve the phases separately. Debangshu et al [14] modeled a single phase stirred-tank reactor and discretized the tank based on the characteristic reaction time scale which showed to capture the essential features of macro mixing. In crystallization Kougoulos et al [15] continued the work by Bermingham, Kramer and ten Cate [16]–[18] by creating compartments with respect to energy dissipation rate, temperature distribution and solid concentration from CFD simulations.

The derived compartment model will be compared to a number of simpler and more complex compartment models to see if the model converges towards a certain number of compartments. The result will thus not be dependent on how it compares to an actual granulator but rather how it compares to similarly derived models.

2. Theory and literature review

This chapter will add some background to wet granulation mechanism as well as the population balance equations for growth and the spray zone. Furthermore it will also cover the kinetic theory of granular flow and the frictional model followed by a more in depth description of compartmental modeling.

2.1 Wet granulation mechanisms

The granulation behavior has been described by a number of different competing mechanisms, but has more recently been condensed into three main areas, summed up in the review by Iveson et al [1]. The first area is wetting and nucleation where the liquid binder is added to the dry powder and distributed throughout the system. The next is consolidation and growth, which handles collisions in the system of primary particles, granules and equipment surfaces. Finally attrition and breakage is considered, where granules break due to collisions with other granules, the impeller or the walls.

Wetting and nucleation mechanisms are considered in the so-called wetting zone where binder liquid comes into first contact with the surface of dry particles. First contact of a droplet with the dry phase is critical for nuclei formation, which depends heavily on the droplet size distribution from the spray. Although other processes, such as mechanical mixing, will change this distribution in the rest of the granulator, focus of initial nucleation in the wetting zone is important to consider. Two key processes in the wetting zone is nuclei formation and binder dispersion [1].

Growth of granules can be considered as two different processes. One is when two granules collide and agglomerate into one larger granules, often referred to as coalescence. The other process that occurs is when a granule comes into contact with a large number of primary particles that stick onto the surfaces of the granule; this is aptly called the layering process. These processes will start as soon as binder liquid is added to the system and will continue well after liquid addition has stopped as long as there are primary particles available.

Consolidation happens when two granules collide and rather than coalesce, they compact, which reduce their size and porosity. Porosity directly controls the strength of the granule and is a key property of granule products, thus it is important to control and optimize. As consolidation occurs it also forces liquid to the surface of the granule, which will increase the likelihood of increased growth. As such it is hard to predict growth due to that consolidation can also alter the properties of the granules.

Breakage is generally put into two different categories, breakage of wet granules into smaller parts and attrition of dried granules back into primary particles. As such, breakage of wet granules will influence the final size distribution of granules and can also be seen as a help to distribute binder liquid more evenly by breaking over-sized granules that contain large amounts of liquid. Attrition of dried granules back into fines is the exact opposite of what the actual process of granulation is to achieve and a situation that should be completely avoided.

These phenomena together control the final property of granule product and becomes quite complicated to control, or model for that matter. Many of these mechanisms require experimental values to be fitted to models used in simulations and simple relations between them to control the final distribution.

2.2 Kinetic theory of granular flows

Kinetic theory of granular flow is a model that tries to describe particle flow as a continuum phase, similarly to a liquid. The derivation is based on the kinetic theory of gases with an extension to non-ideal particle-particle interactions and is first and foremost derived to apply for the rapid regime, which is a dilute system with only binary and instantaneous collisions. Although in high shear granulation there are dense particle regions present with pro-longed, multiple contacts, depicted in figure 1 below to the right.

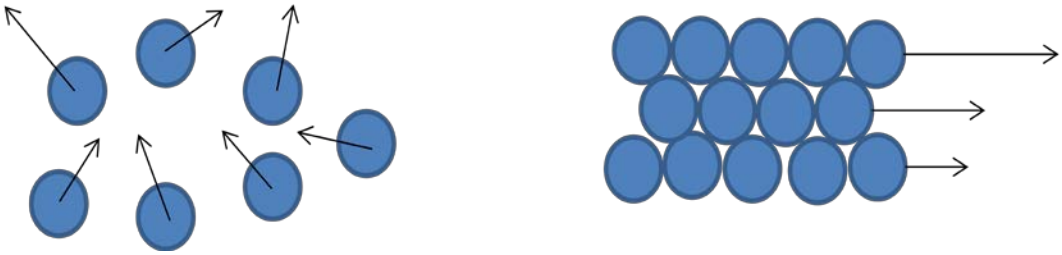

Figure 1. Depiction of two separate regimes present in granular flows. To the left is the dilute, more gas like regime and to the left is the dense regime where multiple contacts between particles are seen.

As an analogue to the thermodynamic temperature in gases there is a granular temperature that similarly describes random movement fluctuations, defined below as

$$\theta = \frac{1}{3}\langle C^2 \rangle \tag{1}$$

Granular temperature is a key property for describing collisions and used in deriving aggregation mechanisms of wet granulation systems seen in the next sub chapter.

To account for both dense and dilute regimes present in the same system, KTGF is normally extended to include a frictional framework. It is assumed that the frictional stress is additive and added to the original KTGF model as extra terms in solid pressure and dynamic solid viscosity. This is quite a heavy simplification and it is also pointed out clearly by Johnson and Jackson in their first paper presenting this extension [19].

2.3 Population balance modeling of granulation processes

Population balance modeling has been used to relate properties such as granule size distribution to the microscopic kinetic properties of the granulation system. So-called kernels are used to describe various mechanisms of the granulation process; as such there are kernels for agglomeration, also called coalescence, as well as kernels for breakage and attrition. Focus, for purposes in this thesis, will be on the aggregation kernel by Tan et al [9]. There will also be nucleation and re-wetting mechanisms present in the population balance to introduce the liquid binder into the system as well as a layering process of primary particles. The two dimensional population balance equation can be seen below in equation 2 and is solved by a constant volume Monte Carlo method developed by Xi Lu [20].

It is outside of the scope of this thesis to examine techniques to solve population balance equations; however different strategies to solve these equations are still very much a relevant topic in granulation. Immanuel and Doyle [21] go through some of the major techniques and also present a robust and efficient strategy for solving higher dimensional equations for granulation processes with good results.

$$\frac{V_i \partial n_i(m_s, m_l, t)}{\partial t}$$
$$= V_i B_0^0 B(m_s, m_l) + V_i R_w^0 R_w(m_s, m_l)$$
$$+ V_i G_0 \frac{\partial n_i(m_s, m_l, t) G(m_s, m_l, t)}{\partial m_s}$$
$$+ \frac{1}{2} V_i \beta_0 \int_0^{m_s} \int_0^{m_l} \beta(m_s, m_l, m'_s, m'_l)\, n_i(m_s - m'_s, m_l$$
$$- m'_l, t) n_i(m'_s, m'_l, t) dm_s dm_l$$
$$- V_i \beta_0 n(m_s, m_l, t) \int_0^{\infty} \int_0^{\infty} \beta(m_s, m_l, m'_s, m'_l)\, n_i(m'_s, m'_l, t) dm'_s dm'_l$$
$$+ \sum_{j=1, j\neq i}^{k} \frac{Q_{i\to j}}{V_i} n_i(m_s, m_l, t) + \sum_{j=1, j\neq i}^{k} \frac{Q_{j\to i}}{V_j} n_j(m_s, m_l, t) \quad (2)$$

where $\boldsymbol{m_s, m_l}$ are the mass in kg of solid and liquid respectively in the granule, V is the compartment volume in $m^3$and Q is flow rate to and from compartments in $\frac{\boldsymbol{m^3}}{\boldsymbol{s}}$. n is the density function, $\frac{\boldsymbol{number\ of\ particles}}{\boldsymbol{kg^2 m^3}}$. G, B, R and β are layering, nucleation, rewetting and aggregation respectively.

2.3.1 Aggregation kernel

The derivation of the aggregation kernel [9] is based on the principles of kinetic theory of granular flow (KTGF) and the equi-partition of kinetic energy (EKE) kernel developed by Hounslow**.** The aggregation kernel can be seen in equation 3 below

$$\beta_{i,j} = \psi g_{i,j} \sqrt{\frac{3\theta_s}{\rho}} (l_i + l_j)^2 \sqrt{\frac{1}{l_i^3} + \frac{1}{l_j^3}} \quad (3)$$

where ψ is the aggregation efficiency, θ_s is the mixture granular temperature which is similar to the description of granular temperature in KTGF

$$\theta_s = \frac{1}{3} m_n \langle C \cdot C \rangle = m_n \theta \quad (4)$$

where m_n is the average mass of a particle and C is the random fluctuating part of the decomposed actual particle velocity from the KTGF. The aggregation kernel consists of one size dependent part, which is the EKE kernel

$$\beta(l_i, l_j) = (l_i + l_j)^2 \sqrt{\frac{1}{l_i^3} + \frac{1}{l_j^3}} \quad (5)$$

and a time dependent part

$$\beta_0(t) = \psi g_0 \sqrt{\frac{3\theta_s}{\rho}} \tag{6}$$

where l is particle size, g_0 the radial distribution function of particle volume fraction defined as

$$g_0 = \left[1 - \left(\frac{\alpha_s}{\alpha_{s,max}}\right)^{1/3}\right]^{-1} \tag{7}$$

Of special interest is the time dependent part of the aggregation kernel, equation 6, which will be calculated from CFD simulations rather than found experimentally. Benefits from actually calculating this is not only that no experiments for the specific granulator are needed, but it is also a way to estimate the actual rate of aggregation in different parts of the system.

2.3.2 Nucleation and re-wetting kernel

Nucleation will happen when a liquid drop comes into contact with a primary particle. Re-wetting occurs when a granule, which by definition will have a certain amount of liquid present, comes into contact with a liquid drop. The initial drop addition rate is described in the following way

$$r_d = \frac{v\dot{M}_{drop}}{\bar{m}_{drop}} \tag{8}$$

where $\dot{M}_{drop}$ is the spray rate in kg/s, $\bar{m}_{drop}$ is the mean mass of droplets in the simulation and v is the volume sample size. Both spray rate and the mean drop size can be determined from experiments and be adjusted depending of what type of spray is present.

The probability of a droplet either re-wetting an existing granule or creating a nuclease by contact with primary particles can be assumed to be proportional to the projected surface area of each population, according to

$$b_0 = \frac{A_p}{A_p + A_g} r_d \tag{9}$$

$$r_w = \frac{A_g}{A_p + A_g} r_d \tag{10}$$

where b_0 is the nucleation rate and r_w is the re-wetting rate. Subscripts p and g is particle and granule respectively with A being the projected area of each population.

2.4 Compartmental modeling

Compartmental, or zonal models has been used for some time to describe systems that have non-ideal mixing within them. An equipment volume is simply divided into a network of compartments that are connected to each other through interconnecting flow rates. The compartment volumes are chosen such that they contain negligible gradients to key controlling properties with respect to mixing.

Many of the mechanisms derived in population balance models are based on the assumption of a well-mixed tank on a unit level scale even though they often have a nonlinear dependency with each other [20]. A compartment model is a way to work around this by defining smaller zones in which this assumption is true.

While CFD is a powerful tool that can solve the hydrodynamic flow field of the granulator; simulations are quite computationally heavy and if they would be augmented with population balance equations as well, the computation time necessary will exceed its usefulness [15]. However if coupled with compartment modeling one can avoid this by separating the hydrodynamic and kinetic parts of the system and quantify them separately. This will allow for a hybrid model in which the hydrodynamic information used in the compartmental model, including interconnected flow rates, volumes and mass fractions of compartments, can be taken directly from the CFD simulations.

One flaw in this approach is that the compartment model does not take into account properties that themselves are functions of conditions in the system, such as granular temperature and how it changes during the granulation process [3]. This could be avoided if the flow field could be updated at various time steps during the granulation process by feeding back information to CFD and thus having a fully interconnected hybrid model. Interesting work has been made in this area by Barrasso et al [22] utilizing DEM simulations connected with PBM. Data transfer between the models occurs at specific conditions, such as if the liquid to solid ratio changes beyond a critical value.

Compartmental modeling has been applied to various types of reactors [12]–[14], [23]–[25]. Depending on what type of process is simulated, for example polymerization, bioreactor or gasification, different types of mechanisms and phenomena drives the process. The process of creating compartments based on computational cells of the CFD simulation differs based on these driving mechanisms. Normally one or more properties of interest for the system is identified and used as a criterion for aggregation of cells to construct a compartment. Depending on which type of phenomena that is of importance for the process, different choices are made. For bioreactors it was shown that viscosity was important for the mass transfer of oxygen in the system. Viscosity also tends to vary over the tank, both spatially and temporally. Viscosity is thus a key parameter in this system and each compartment was constructed such that with respect to viscosity the compartment was well-mixed. This general procedure was done similarly in a stirred-tank reactor however the residence time of the reaction was used to separate the compartments. In a gasification process a different process was employed in which the combustion and gasification phases were separated by compartments.

Crystallization is a process that is somewhat similar to granulation and compartmental modeling has been used successfully [15], [16], [18]. Specifically three parameters were used for compartmentalization of the crystallizer volume. Each compartment were to have negligible gradients with respect to local energy dissipation rate, temperature distribution and solids concentration [15].

Studies has also been made in powder mixing by Portillo et al. [26] utilizing compartmental modeling. They use a pure compartment model rather than combining it with any hydrodynamic modeling to try and characterize powder mixing by discretizing a vessel into a number of homogenous subsections and described the mass flux of particles that enter and leave the compartment as a random process. What could be seen was a very efficient model with regard to computational time while allowing for a large number of particles.

Similarly to the work done in crystallization a first attempt to compartmentalize a high shear granulator were done by Xi Yu [20]. With similar heuristics as was used for a crystallizer [16], a simple method of finding compartments for high shear granulation was realized.

3. Methodology

The method used to realize the compartment model is based on a CFD simulation of the high shear granulator. With the general picture of the flow field and information on solid volume fraction and granular temperature one can start to discretize the CFD grid into compartments. To aid in this process, cell data was extracted from CFD and examined in MatLab.

The general method used here will follow a separation of cells based on a sorting mechanism. By starting from the highest value in the system with regard to granular temperature for example, and finding all similar values within a set interval. The interval can be set using a tolerance $\tau < 1$ such that

$$Find(P) = Max(P) * \tau \tag{11}$$

Where P is any property of interest in the system. Coordinates in space is extracted along with the value and if cell values are adjacent to each other a compartment can be separated.

Properties that is important for the granulation process includes volume fraction and granular temperature. Both of these are critical for how growth of granules evolve over time. Further the time dependent part of the aggregation kernel, β_0, is a function of both volume fraction and granular temperature and will be used as the critical parameter of choice to determine compartments.

Collection of volumes, solid volume fraction, β_0 and interconnected flow rates for all compartments are done by a user defined function (UDF) in Fluent. This is done over a time period of 1 second to account for variations in the system.

3.1 CFD model

CFD simulations has been carried out in Ansys Fluent 13 based on work of Xi Yu [20]. The system is based on a laboratory scale DIOSNA high shear granulator with a volume of 4 liter with a three bladed beveled impeller rotating at 600 rpm.

The lower part of the geometry is the rotating region, in which the impeller is rotated by a sliding mesh technique. This means that the upper part of the geometry is static and the lower part rotates and the momentum in the interface of these two regions are matched in each time step. Both of the regions are illustrated in figure 2 below.

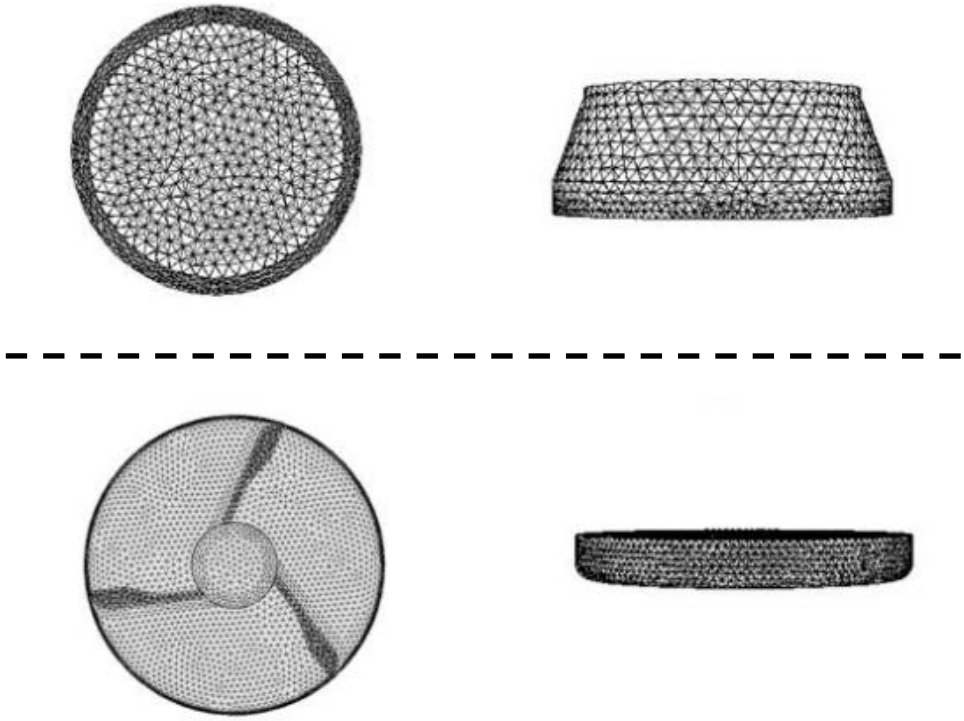

Figure 2. Side and top view of the two regions in the granulator. Above the dashed line is the static part and below is the rotating part.

The geometry and mesh is based on the work by Darelius [27]. To the left is a top view and to the right is a side view of the two regions. The solid material used in the simulations is based on microcrystalline cellulose (mcc) with a diameter of 59 microns for a total of 300 g in the simulation. A time step of 0.0007 seconds with 150 iterations per time step is used with quite low relaxation factors to achieve a converged solution.

3.2 Investigation of CFD results

Compartmentalization is done in a step by step type of way. First compartments are selected to represent the overall flow pattern of the granulator, which is done by inspection of dimensions and geometry of the vessel. Secondly the spray compartment is missing from the actual CFD simulation and must be estimated in another way.

Compartments found after the first step will be further separated based on gradients in the time dependent part of aggregation kernel, seen in chapter 2.3 equation 6, with ψ equal to unity. After this special care will be put into how the connection between compartments look because of the difficulties in implementing a moving surface through the UDFs in Fluent.

Figure 3 shows contour plots of the volume fraction in the granulator; what can be seen is a good representation on how the flow field looks like inside the system. A large void with is located at the center where the volume fraction is lower than 0.01. A maximum bed height is also located at the upper part in the granulator. Based on this, a domain of interest in which most of the solid phase is located can be established.

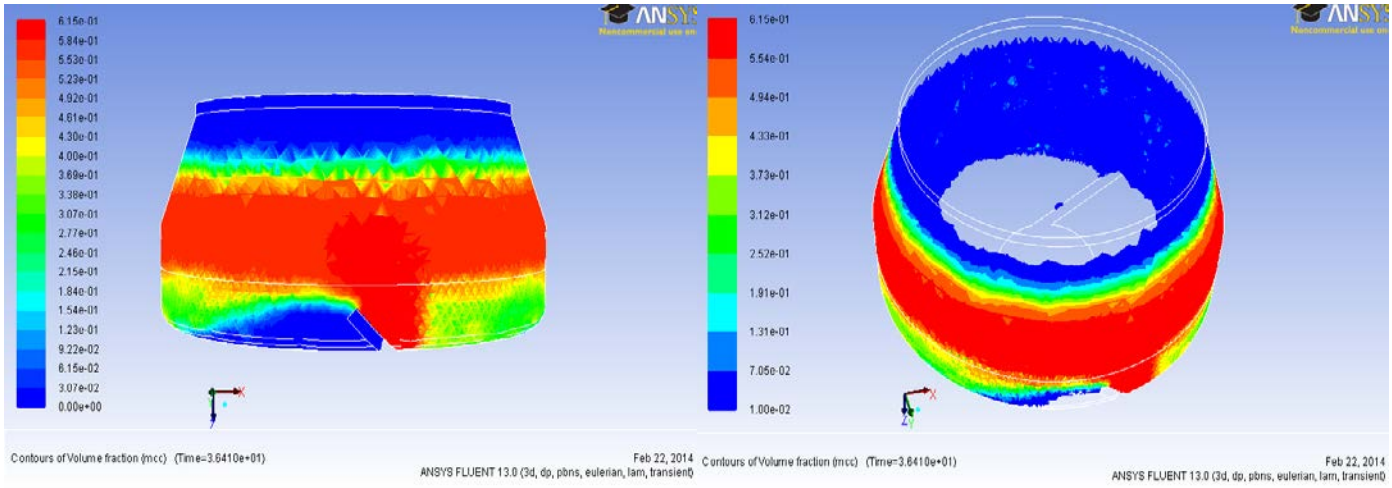

Figure 3. Two different views of volume fraction larger than 0.01 plotted as contours.

In figure 4 the volume fraction can be seen from a top view from extracted data in MatLab. Particles tend to accumulate closer to the walls of the system and create a void in the center of the granulator. The radius from origin to the critical volume fraction of 0.01 is found to be equal to 0.8 mm, as indicated by an arrow in figure 4.

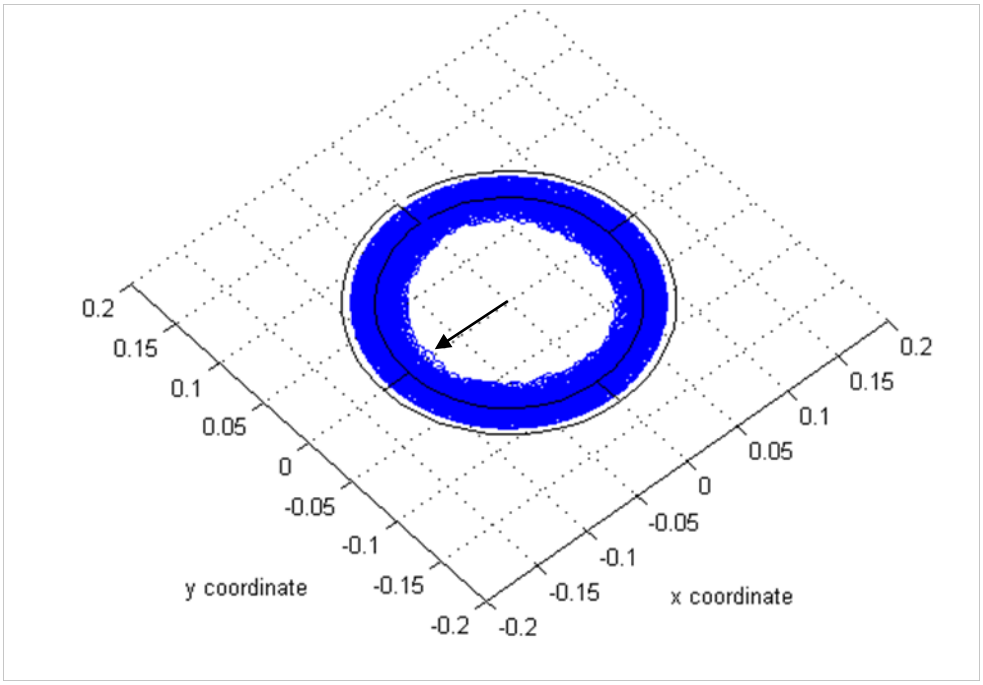

Figure 4. Showing the location of cells that contain 0.01 up to a maximum of 0.62 volume fraction. Coordinate axis are distance in meters.

The critical radius found above will determine in which region we start our compartmentalization, as this will determine the two first compartments in the top and bottom part of the granulator. Further on, all the compartments created in the bottom part will have the same height. This height is what separates the moving mesh to the static part and is found to be 0.3 meters, which can be seen in figure 5.

As well as the critical radius that can be found for the majority of the particles in the system, a maximum height is also found in the granulator. This is the top of the bed and will also be used to limit the compartments located in the upper part of the granulator. The bed height, equal to 0.91 m, can be seen illustrated in figure 3 to the right.

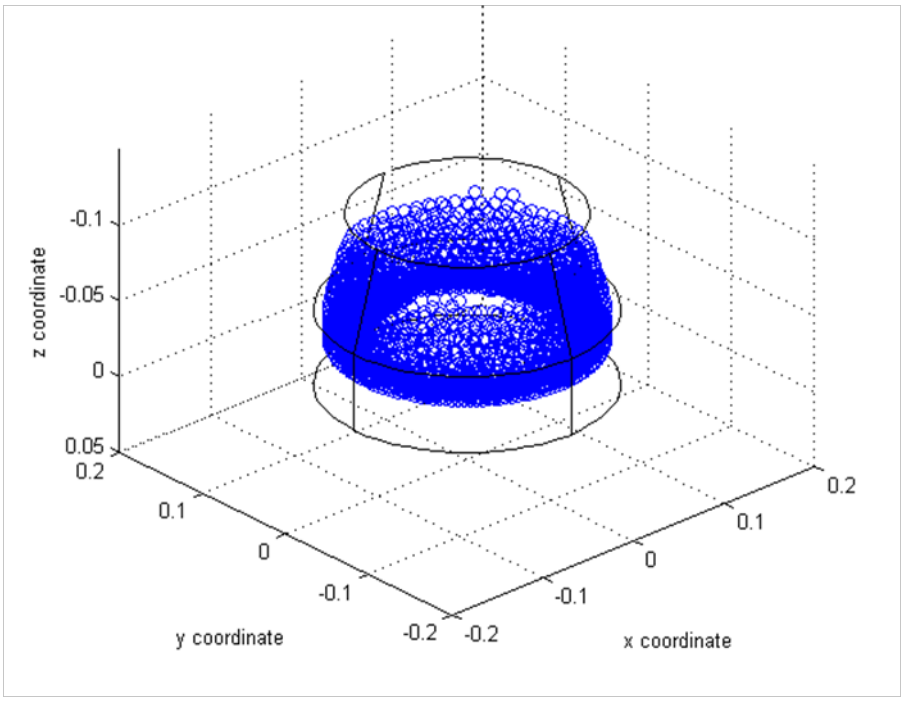

Figure 5. Location of cells that contain volume fraction above 0.01 in the top part of the granulator. Coordinate axis are distance in meters.

As such there is two critical distances in which most of the particles are contained and which will be the base for the volume. With this approach we account for approximately 96 % of the mass in the system. This is also illustrated in figure 6 were the mass of particles are shown with respect to the volume fraction, where the larger part of the mass is located in the more dense regions of the granulator.

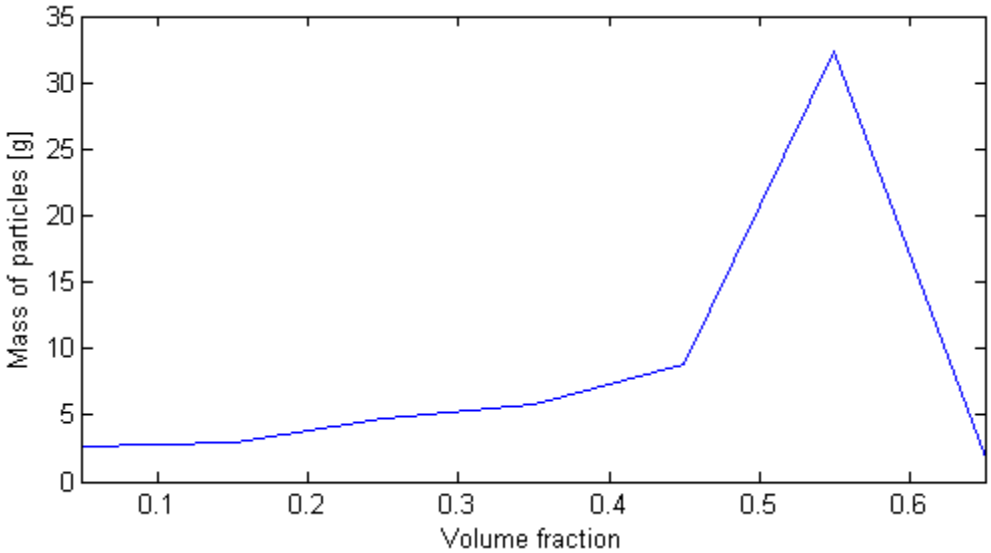

Figure 6. Distribution of the total mass in the system versus the corresponding volume fraction.

Further investigation of β_0 with respect to volume fraction, there is an increase, as should be, with higher volume fraction. There is also a larger variation as volume fraction increase, which can be seen in figure 7. For granular temperature there is a larger variation for β_0, this is due to that granular temperature can still be high even though volume fraction is low and vice versa.

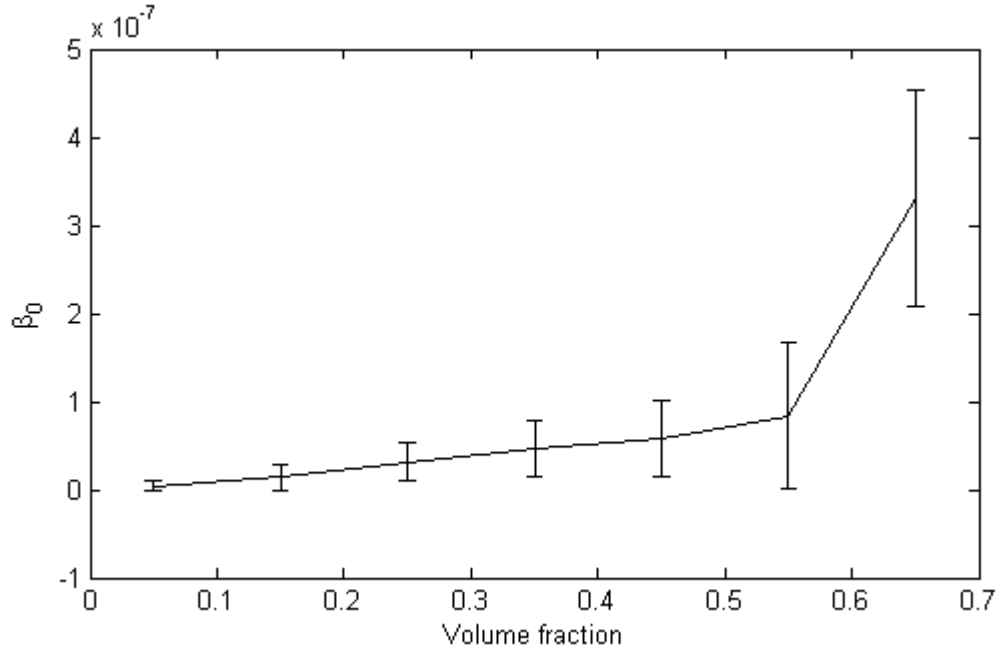

Figure 7. β_0 plotted versus volume fraction. Variation in β_0 is shown as error bars around an average span of volume fraction.

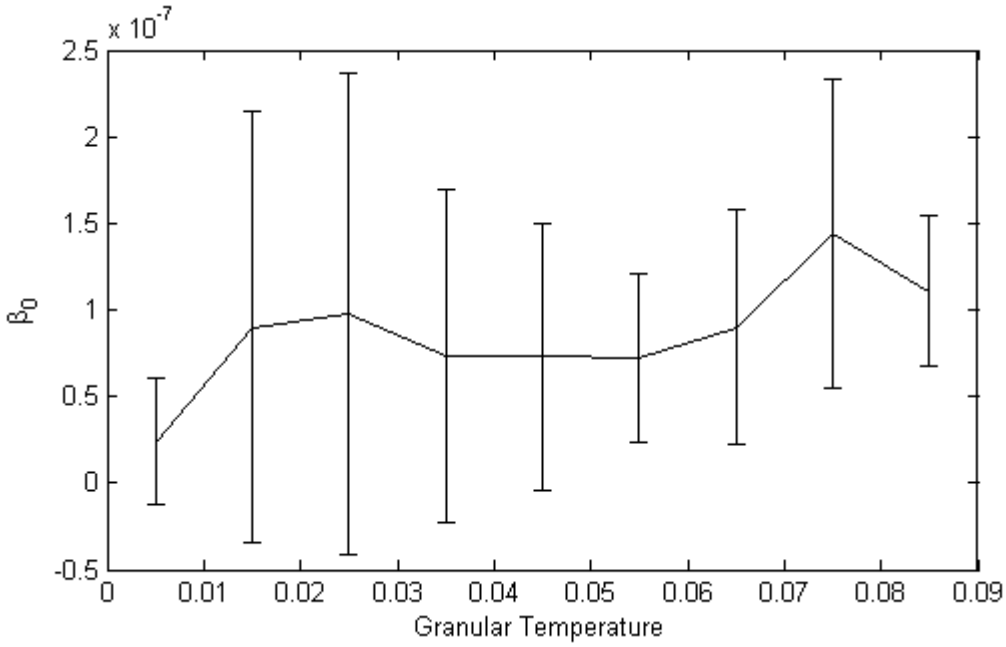

Figure 8. β_0 plotted versus granular temperature. Variation in β_0 is shown as error bars around an average span of granular temperature.

Continuing compartmentalization based on β_0 results in one distinct compartment located on each of the impeller blades, seen in figure 9. In this region, both volume fraction and granular temperature are high which directly correlates to a high β_0. This can be seen as a high collision region with extra force applied by the impeller blade.

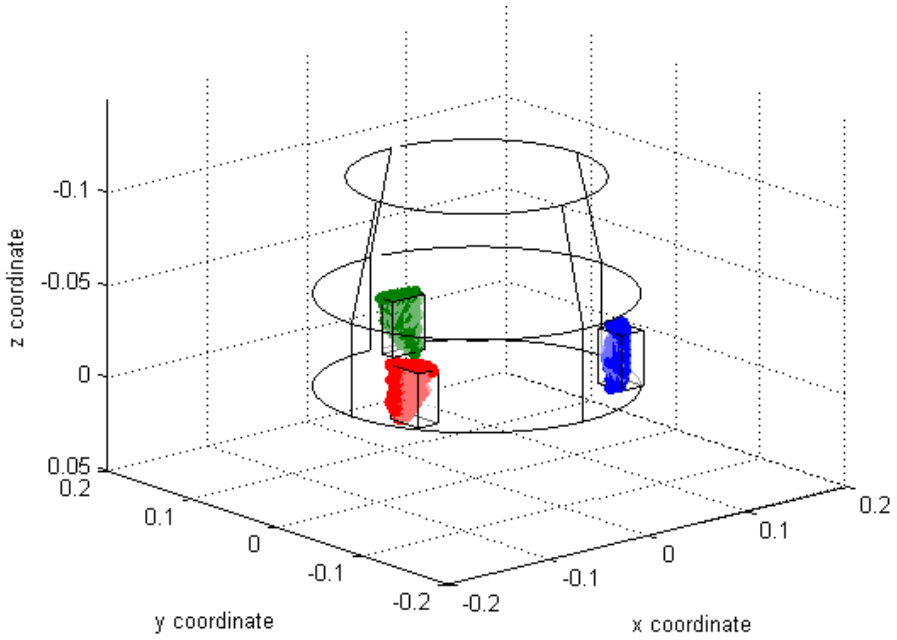

Figure 9. Impeller compartments separated based on β_0. Coordinate axis are distance in meters.

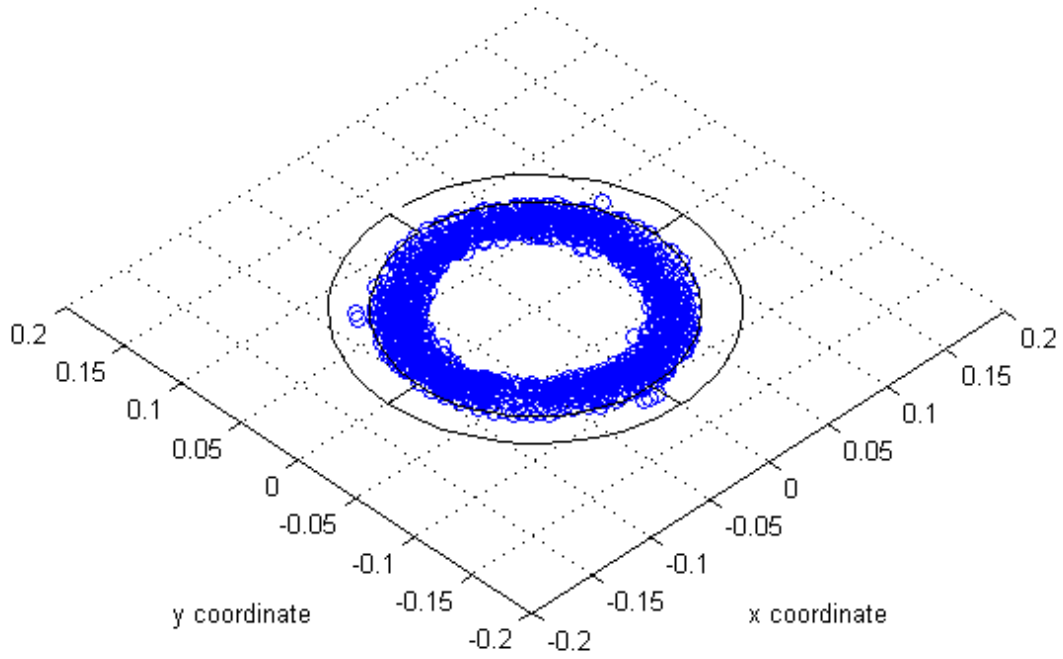

Figure 10. Two separated ranges of β_0. In the right figure indents can be seen in three places which are where the impeller compartments have been separated from. Coordinate axis are distance in meters.

Finding other distinct connected compartments is difficult due to the even distribution of β_0 over a large part of the granulator. However in the lower end of the spectrum there is a slight separation towards the center, seen in figure 10, but the difference between them is very slight and can probably be considered insignificant, at least compared to the impeller compartment.

3.2 UDF implementation in Fluent

A user-defined function, UDF, is a function that is programmed in C that can be loaded into Fluent to enhance the basic features of the program. Here it will be used to collect flow rates between the compartments and also find the average properties of the compartments, such as volume fraction, granular temperature and β_0. It is especially useful when a time averaged value is needed, as there is no need to re-create surfaces manually for every time step while re-calculating the position depending on the impeller movement.

Two different approaches were investigated to create a surface in the UDF. Both methods use cell-centered values that are collected from cells in the surface. To calculate the volumetric flow rate the velocity is taken from the cell and is calculated as in equation 12 below

$$Q = \int \alpha_s \, (u_s - r\omega) dA \tag{12}$$

where u_s is the velocity of the particle phase, r is the radius and ω is the angular velocity of the rotating compartments in the lower part of the granulator.

The first method use a built in search macro, found in cxndsearch.h in the fluent directory. The macro searches for a cell in a geometrical point in space when supplied with x, y and z coordinates. Supplied with an expression for a surface the UDF locates the right cell based on the geometrical point and calculates the flow rate over it based on the velocity. The direction of the flow is determined based on it the calculated flow rate is positive or negative and thus the flow rate to and from compartments is found. Due to that each point has to be calculated individually and then provided for the macro to perform a search, this particular method is quite slow. However, even if small steps between calculated points are used, the macro still fails to capture the whole surface seen in figure 11 below.

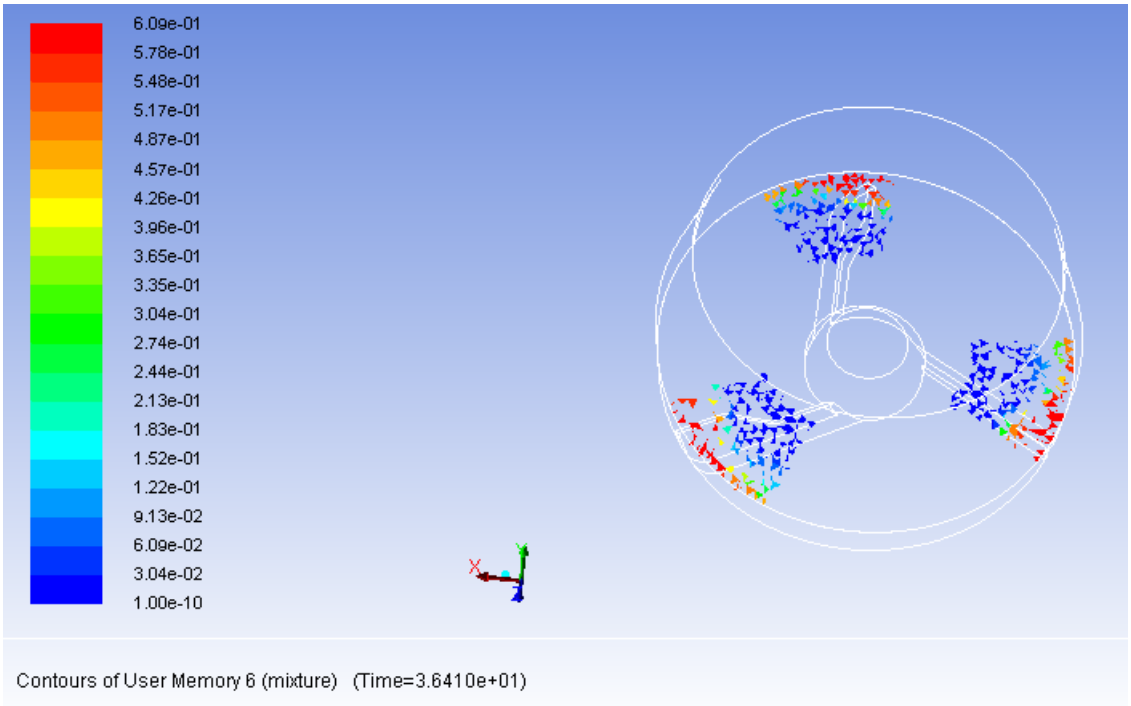

Figure 11. The scatter like surface created with the supplied search macro in cxnd search in Fluent.

The second method uses another Fluent macro that loops through all cells rather than using specific geometrical points to find the cell. Using the cell centroid coordinate to separate a small segment where the surface is located, volumetric flow rate can be collected. This turns out to be a lot faster and more efficient than the first method, mostly due to the amount of search points that has to be supplied to the first macro. Since all cells are looped through there is no risk of missing adjacent cells.

The UDF can build horizontal, vertical and cylinder surfaces. It is difficult to do surfaces with slopes or other shapes due to the tetrahedral mesh. The total area is calculated beforehand and is divided by the total number of cells that the surface contains. This gives a rough but still good estimate of the flow rate when compared to a real surface created with the surface tool in Fluent. An example of the interconnected surfaces created by the UDF can be seen in figure 12 below.

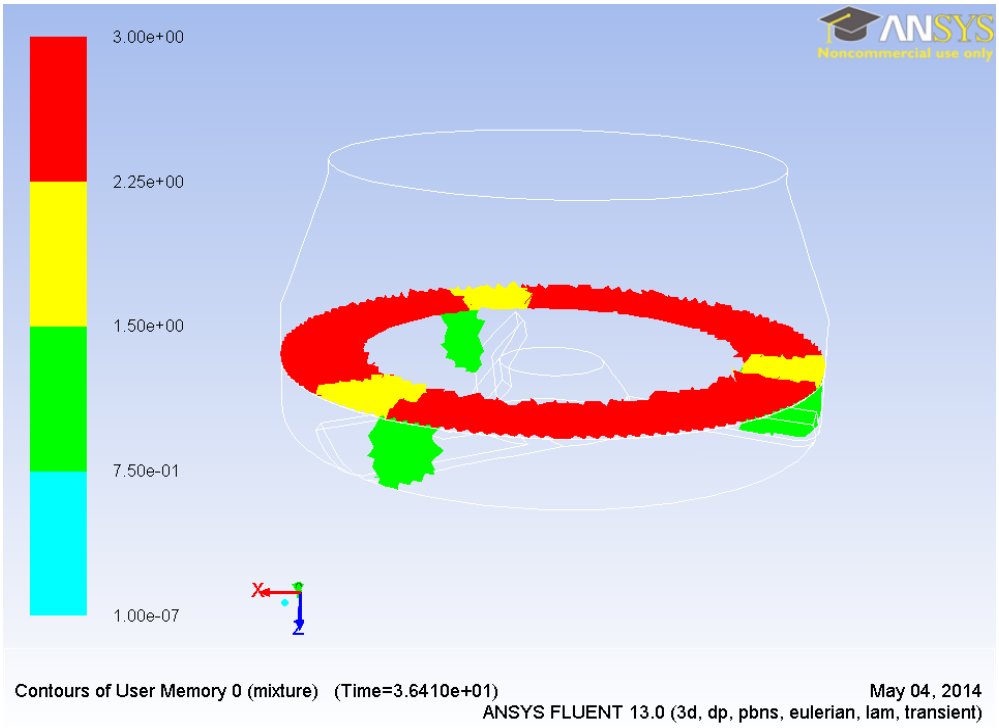

Figure 12. Surfaces created with the looping macro in Fluent.

Besides collecting flow rates from and to compartments the UDF also collects volume averaged values of the mentioned compartments. Time averaged values spanning over 1 second which corresponds to 10 impeller revolutions has been used. 1 second has been deemed satisfactory based on a longer test of collecting flow rates to see the variations in the system. A variation of ± 3 % from the mean was found, as illustrated in figure 13.

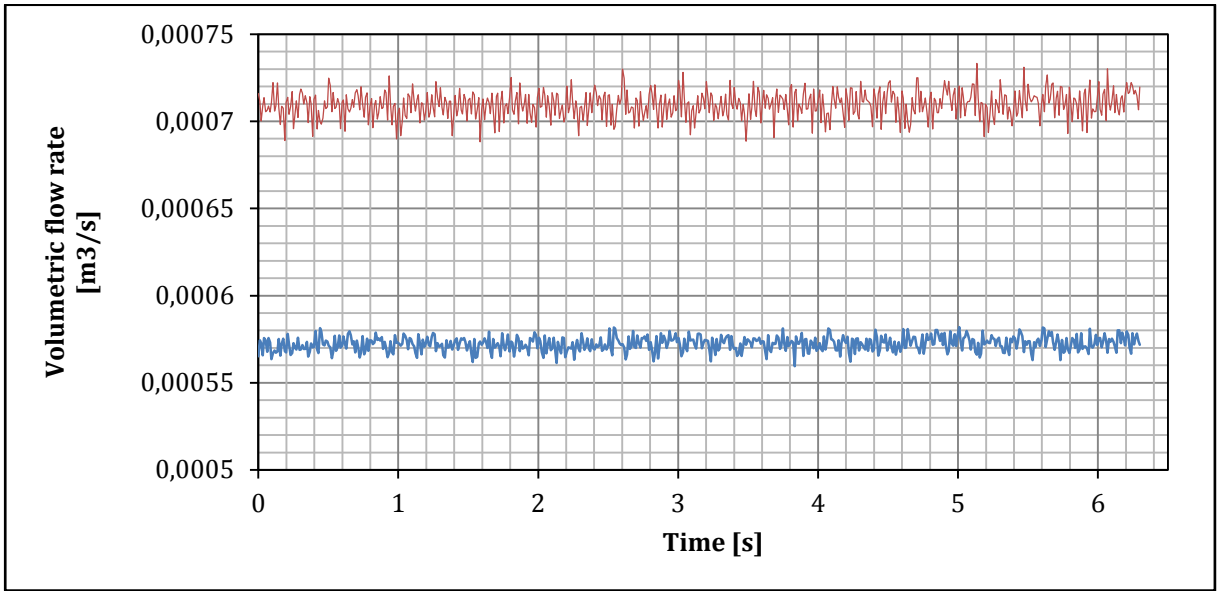

Figure 13. Test to see variations in the granulator over time. Flow rates are taken arbitrarily.

4. Results

The results are separated into two parts. The first covers the compartmentalization of the granulator and the different cases and the second part shows results from the population balance coupled compartment model.

4.1 Compartmentalization

A base case have been constructed based on the results from the CFD simulation and built on this base case are five more cases that range from simpler builds to more complex, to ensure that a good model has been found. General information of the cases is found in table 1 for specific data and flow rates for all cases see table 2 and table 3 in appendix 1.

Table 1. General information on the 6 constructed compartment models

	Number of compartments	Comment
Case 1	2	Whole granular volume as one compartment.
Case 2	2	Void in center removed, still one compartment.
Case 3	3	Geometrical separation of static and rotating part.
Case 4	4	The base case with the impeller compartment.
Case 5	5	One further separation of the larger compartment in the lower part.
Case 6	7	Cylindrical surface towards the center.

The first case is the simplest construction of compartments, i.e. the whole granulator volume and the sixth and last case is the most complex. In all of the cases; compartment 1 is the spray compartment. The spray compartment is based on Xi Yu's [20] assumptions, calculations and experimental values that are assumed to apply for a common spray found in high shear granulation equipment.

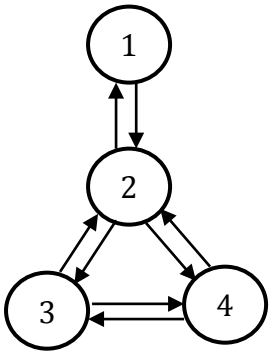

Figure 14. Connectivity diagram of the flow rates to and from compartments for case 4.

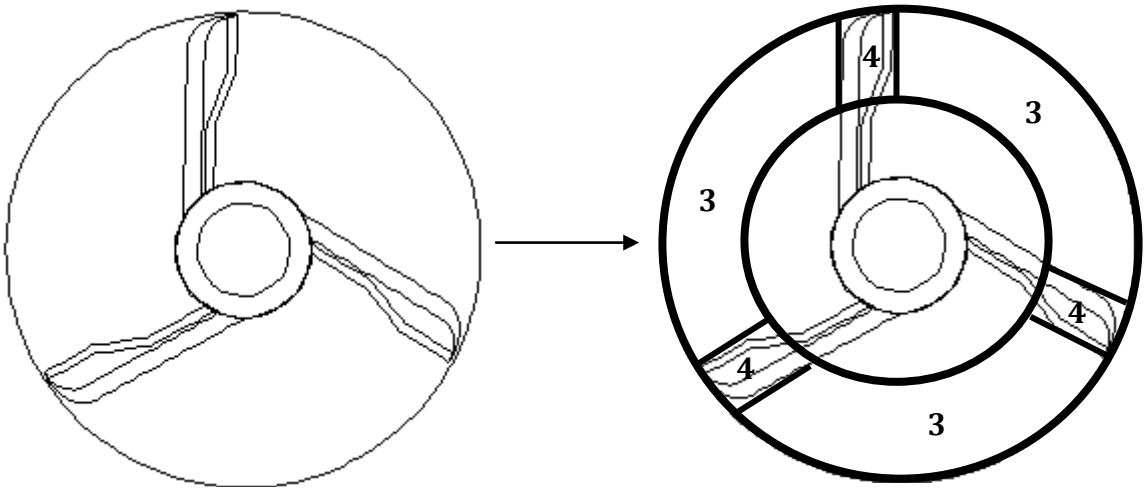

Figure 15. Top view of the lower part of the granulator illustrating compartment 2 and 3 for the base case.

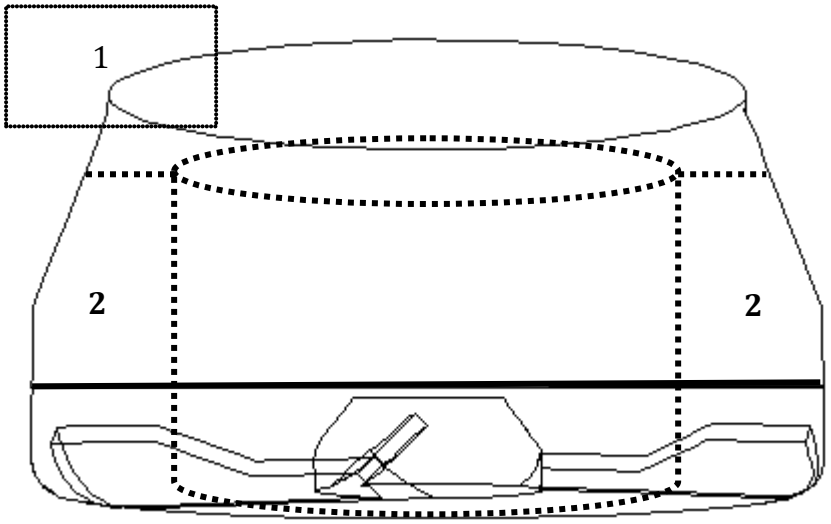

Figure 16. Side view of the whole granulator illustrating compartment 2 in the upper part as well as the fictive spray compartment numbered as 1.

In case 2 the large empty space is neglected and is treated as single compartment, essentially the same as case 1 but with a smaller volume. Case 1 & 2 are unique as they do not have any flow rates calculated from the CFD simulation, only mean data on volume fraction and β_0 are extracted.

Case 3 is the natural separation of the rotating part to the static. This is necessary for calculating the flow rates correctly as the movement of the impeller is modeled as moving mesh, and thus the cells themselves move.

The base case includes the impeller compartment, which in chronological order of simpler to complex, is case 4 illustrated in figure 15 and figure 16. This compartment

exhibit high particle load as well as high granular temperature, an indication of a high aggregation compartment.

The last two cases, 5 and 6, are further separations of case 4 to see if the solution converge, a sort of mesh independence test. Case 5 divides compartment 2 in figure 15 into two separate compartments, yielding 5 total compartments. Case 6 divides all compartments by a cylindrical surfaces based on the slight gradient found towards the middle of the granulator.

4.2 Population balance results

First run of the model is with a pre-defined value for β_0, which is the same in all compartments, that is based on previously done experiments and simulations by Xi Lu. This yields the results shown in figure 17 on the particle size distribution. There is a clear separation of the first case compared to the others where no significant difference can be seen.

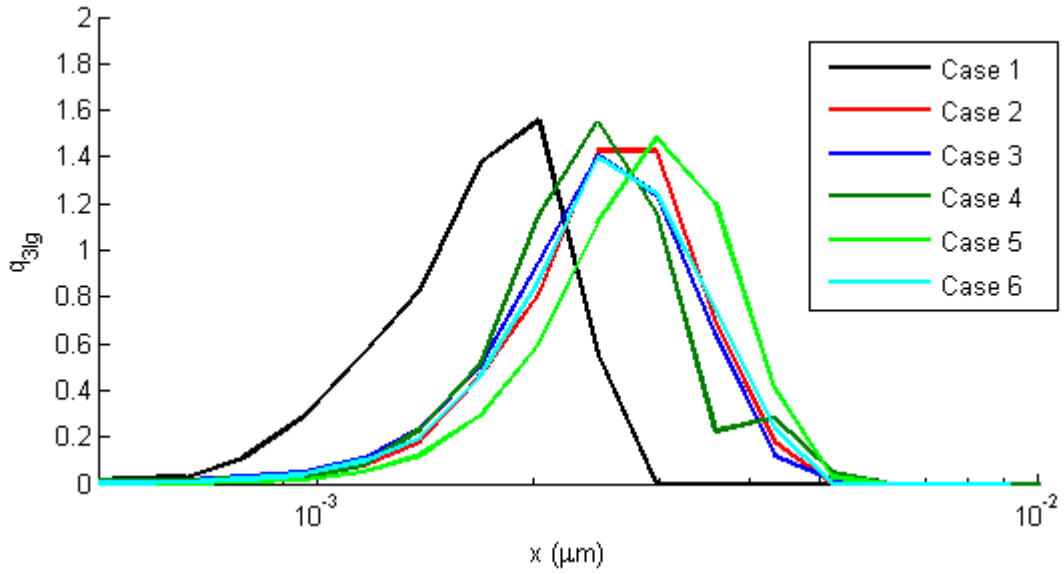

*Figure 17. Granulation size distribution for the six cases after 5 minutes with β0 = 1*10-9.*

However after applying the calculated values for β_0, the differences become much harder to discern, as seen in figure 18.

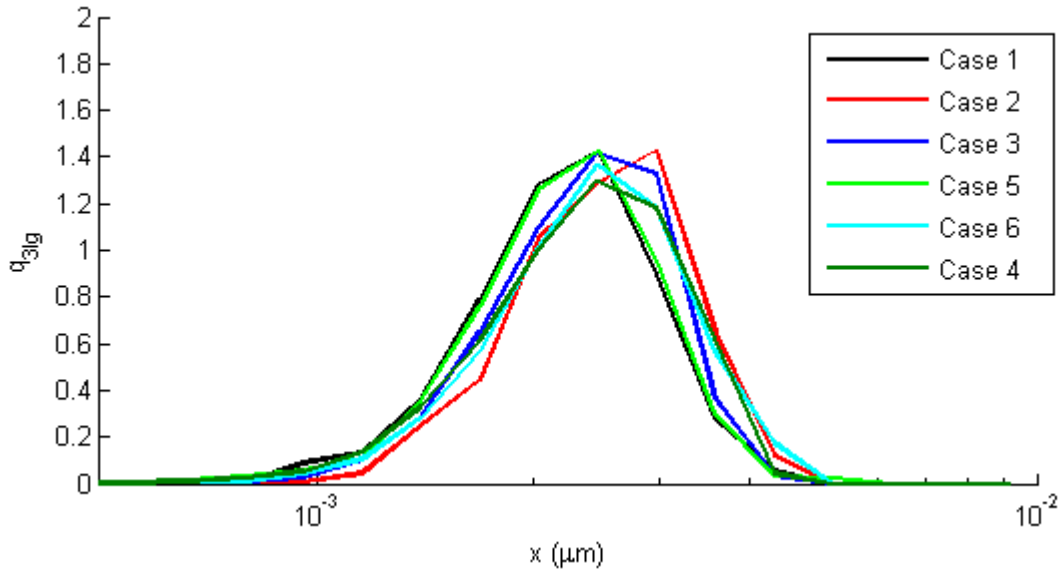

Figure 18. Granulation size distribution for the six cases after 5 minutes with β_0 calculated from CFD.

5. Discussion

Creating compartment volumes in Fluent with an automatic procedure is quite limited. It could of course be done manually; however this would require re-creating them for every time step as the mesh rotates. Considering a process in which time-averaging is of less importance, the manual approach might be worth considering; on the other hand there is still the re-creating manually if more than one case is considered. This is only considering surfaces for flow rates, considering volume averaged values for volume fraction and similar properties it might be require re-modeling of CAD design to add the compartments. Re-compartmentalization would again be a nuisance and best be avoided.

A large assumption in the compartment creation is to remove, or rather neglect the large middle column of the granulator. It is based on the very small amount of mass present in a very large volume and that the interaction of particles in this part should be trivial. Also when considering average values over the whole granulator this would give a false indication of for example volume fraction since it is more or less zero in most of granulator and close to 0.5 at the walls. This indirectly makes a simplification for the flow rate calculations, as the flux in the center is close to zero as well, which means that one less surface needs to be created in Fluent.

The results in figure 17 and figure 18 indicate that the compartments for this particular granulator might be superfluous and the granulator can indeed be considered to be well mixed. An indication for this is the high flow rates of particles between the compartments. Pushing the model further to visualize the effect of flow rates a scaling test was done in order to see when the compartment model started to deviate from the results above. The result is shown below in figure 19 where the flow is scaled down by a factor 50. From this we can see that cases with more compartments are affected to a much greater degree than cases with fewer. The main cause for this is probably the time

it takes for primary particles and liquid drops to meet in the system and coalesce. When they do meet and start to coalesce, they also start to aggregate by collisions within the same compartment rather than moving around as freely with higher flow rates, leading to the large granules relative to the results above. This is also an effect of not having a breakage kernel present in our model; this would otherwise be a way of controlling the size with a breakage criterion for a specific size.

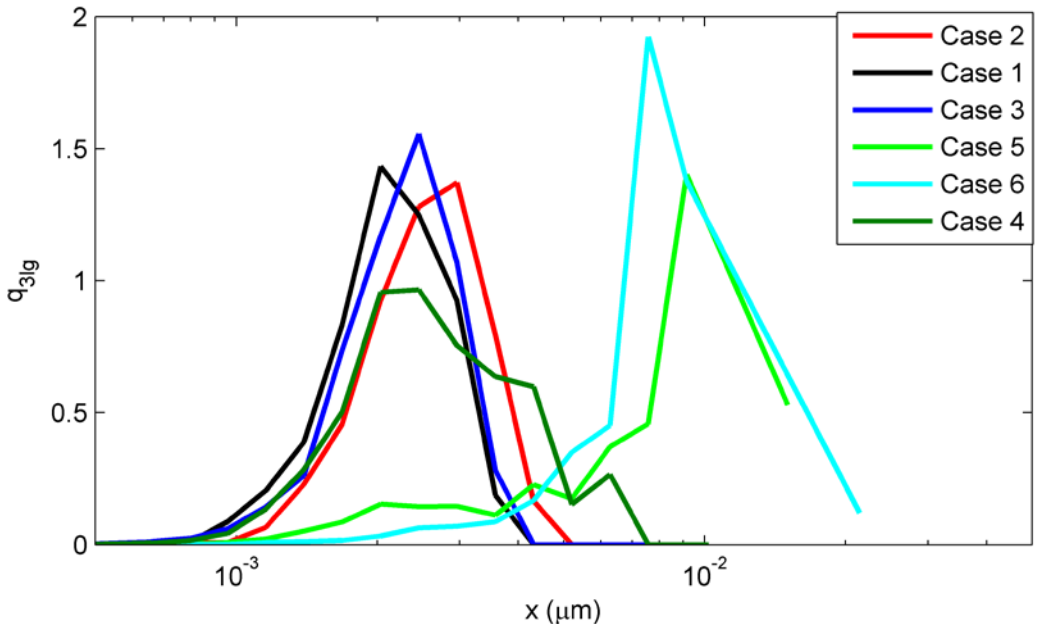

Figure 19. Granulation size distribution for the six cases with the flow rates scaled down by 50.

The impeller speed would have to be lower to achieve a smaller flow rate which would change flow field and also change the compartment layout, so it still hard to draw definite conclusions from this for a higher limit of the flow rate when compartments might be a necessity.

6. Conclusion and future work

An efficient code in the form of a user defined function in Fluent to collect flow rates over surfaces and collect information in compartment volumes has been achieved. It is specific for cylinders and can be used for vertical, horizontal and cylindrical surfaces. A method for finding coordinates for surfaces and volumes has been made based on gradients in the system, specifically volume fraction and granular temperature and the time dependent coefficient in the aggregation kernel β_0.

It is seen that for the granulator in question, spatial compartment modeling is not necessarily needed in the sense of this not being a well-mixed system. However further work to include more mechanism such as breakage and fine tuning parameters in the population balance is still of interest. Using compartmental modeling for the spray zone seems to be a promising idea and further work to include the chopper might also be of interest.

A temporal compartmentalization of the different stages of the granulation process with or without spatial compartment modeling is also of interest to update the population balance with the changing flow field over time. This was done to a certain degree by Barrasso et al [22] on a smaller scale, however to do this on a larger unit scale can be of great interest for scale-up operation.

6. References

[1] S. M. Iveson, J. D. Litster, K. Hapgood, and B. J. Ennis, "Nucleation, growth and breakage phenomena in agitated wet granulation processes: a review," *Powder Technol.*, vol. 117, no. 1–2, pp. 3–39, Jun. 2001.

[2] A. M. Nilpawar, G. K. Reynolds, A. D. Salman, and M. J. Hounslow, "Estimating aggregation efficiency from observation of flow behaviour in a high shear mixer," pp. 1–10.

[3] F. Bezzo and S. Macchietto, "A general methodology for hybrid multizonal/CFD models Part I. Theoretical framework," *Comput. Chem. Eng.*, vol. 28, no. 4, pp. 513–525, Apr. 2004.

[4] A. Darelius, A. Rasmuson, B. van Wachem, I. Niklasson Björn, and S. Folestad, "CFD simulation of the high shear mixing process using kinetic theory of granular flow and frictional stress models," *Chem. Eng. Sci.*, vol. 63, no. 8, pp. 2188–2197, Apr. 2008.

[5] B. H. Ng, Y. L. Ding, and M. Ghadiri, "Modelling of dense and complex granular flow in high shear mixer granulator—A CFD approach," *Chem. Eng. Sci.*, vol. 64, no. 16, pp. 3622–3632, Aug. 2009.

[6] P. J. Abrahamsson, I. N. Björn, and a. Rasmuson, "Parameter study of a kinetic-frictional continuum model of a disk impeller high-shear granulator," *Powder Technol.*, vol. 238, pp. 20–26, Apr. 2013.

[7] M. Khalilitehrani, P. J. Abrahamsson, and A. Rasmuson, "The rheology of dense granular flows in a disc impeller high shear granulator," *Powder Technol.*, vol. 249, pp. 309–315, Nov. 2013.

[8] L. X. Liu, J. D. Litster, G. Associates, and H. H. Road, "Coalescence of Deformable Granules in Wet Granulation Processes," vol. 46, no. 3, pp. 529–539, 2000.

[9] H. S. Tan, M. J. V. Goldschmidt, R. Boerefijn, M. J. Hounslow, a. D. Salman, and J. a. M. Kuipers, "Building population balance model for fluidized bed melt granulation: lessons from kinetic theory of granular flow," *Powder Technol.*, vol. 142, no. 2–3, pp. 103–109, Apr. 2004.

[10] A. Darelius, A. Rasmuson, I. N. Björn, and S. Folestad, "High shear wet granulation modelling—a mechanistic approach using population balances," *Powder Technol.*, vol. 160, no. 3, pp. 209–218, Dec. 2005.

[11] F. Bezzo and S. Macchietto, “A general methodology for hybrid multizonal/CFD models Part II. Automatic zoning,” *Comput. Chem. Eng.*, vol. 28, no. 4, pp. 513–525, Apr. 2004.

[12] F. Bezzo, S. Macchietto, and C. C. Pantelides, “General hybrid multizonal/CFD approach for bioreactor modeling,” *AIChE J.*, vol. 49, no. 8, pp. 2133–2148, 2003.

[13] I. Iliuta, A. Leclerc, and F. Larachi, “Allothermal steam gasification of biomass in cyclic multi-compartment bubbling fluidized-bed gasifier/combustor - new reactor concept.,” *Bioresour. Technol.*, vol. 101, no. 9, pp. 3194–208, May 2010.

[14] D. Guha, M. P. Dudukovic, P. A. Ramachandran, C. Reaction, and S. Louis, “CFD-Based Compartmental Modeling of Single Phase Stirred-Tank Reactors,” vol. 52, no. 5, 2006.

[15] E. Kougoulos, a. G. Jones, and M. Wood-Kaczmar, “CFD Modelling of Mixing and Heat Transfer in Batch Cooling Crystallizers,” *Chem. Eng. Res. Des.*, vol. 83, no. 1, pp. 30–39, Jan. 2005.

[16] S. K. Bermingham, H. J. M. Kramer, and G. M. van Rosmalen, “Towards on-scale crystalliser design using compartmental models,” *Comput. Chem. Eng.*, vol. 22, pp. S355–S362, 1998.

[17] H. J. M. Kramer, J. W. Dijkstra, A. M. Neumann, R. Meadhra, and G. M. Van Rosmalen, “Modelling of industrial crystallizers , a compartmental approach using a dynamic flow-sheeting tool,” vol. i, pp. 1084–1088, 1996.

[18] A. ten Cate, S. K. Bermingham, J. . Derksen, and H. J. M. Kramer, “Compartmental modeling of an 1100L DTB crystallizer based on Large Eddy flow simulation,” *10th Eur. Conf. Mix.*, pp. 255–264, 2000.

[19] P. Abrahamsson, “Continuum modeling of particle flows in high shear granulation,” Chalmers University of Technology, Department of Chemical and Biological Engineering, Gothenburg, 2012.

[20] X. YU, “An in-silico model of granulation,” University of Sheffield, 2012.

[21] C. D. Immanuel and F. J. Doyle, “Solution technique for a multi-dimensional population balance model describing granulation processes,” *Powder Technol.*, vol. 156, no. 2–3, pp. 213–225, Aug. 2005.

[22] D. Barrasso, J. Li, K. Debus, R. Aglave, T. Eppinger, R. Ramachandran, and S. Bermingham, “Multi-scale modeling of powder processes:,” pp. 1–29, 2014.

[23] A. H. Alexopoulos, P. Pladis, and C. Kiparissides, “Nonhomogeneous Mixing Population Balance Model for the Prediction of Particle Size Distribution in Large Scale Emulsion Polymerization Reactors,” *Ind. Eng. Chem. Res.*, vol. 52, no. 35, pp. 12285–12296, 2013.

[24] Y. Le Moullec, C. Gentric, O. Potier, and J. P. Leclerc, “Comparison of systemic, compartmental and CFD modelling approaches: Application to the simulation of a biological reactor of wastewater treatment,” *Chem. Eng. Sci.*, vol. 65, no. 1, pp. 343–350, Jan. 2010.

[25] M. Gresch, R. B. R. U, A. Meyer, and W. Gujer, “Compartmental Models for Continuous Flow Reactors Derived from CFD Simulations,” *Environ. Sci. Technol.*, vol. 43, no. 7, pp. 2381–2387, 2009.

[26] P. M. Portillo, F. J. Muzzio, and M. G. Ierapetritou, “Characterizing powder mixing processes utilizing compartment models.,” *Int. J. Pharm.*, vol. 320, no. 1–2, pp. 14–22, Aug. 2006.

[27] A. Darelius, A. Rasmuson, B. van Wachem, I. Niklasson Björn, and S. Folestad, “CFD simulation of the high shear mixing process using kinetic theory of granular flow and frictional stress models,” *Chem. Eng. Sci.*, vol. 63, no. 8, pp. 2188–2197, Apr. 2008.

Appendix 1. Compartment data

Table 2. Compartment properties for all cases.

	Case 1		
	Volume [m3]	Volume fraction solid	β_0 [m/s]
Compartment 1	0,000020	0,30	0
Compartment 2	0,0016	0,26	5,0E-06
	Case 2		
	Volume [m3]	Volume fraction solid	β_0 [m/s]
Compartment 1	0,000020	0,30	0
Compartment 2	0,0039	0,10	2,1E-06
	Case 3		
	Volume [m3]	Volume fraction solid	β_0 [m/s]
Compartment 1	0,000020	0,30	0
Compartment 2	0,0010	0,34	5,0E-06
Compartment 3	0,00056	0,11	5,1E-06
	Case 4		
	Volume [m3]	Volume fraction solid	β_0 [m/s]
Compartment 1	0,000020	0,30	0
Compartment 2	0,0010	0,34	5,0E-06
Compartment 3	0,00048	0,08	2,7E-06
Compartment 4	8,1E-05	0,28	1,9E-05
	Case 5		
	Volume [m3]	Volume fraction solid	β_0 [m/s]
Compartment 1	0,000020	0,30	0
Compartment 2	0,0010	0,34	5,0E-06
Compartment 3	0,00035	0,08	2,6E-06
Compartment 4	0,00012	0,09	3,2E-06
Compartment 5	8,1E-05	0,28	1,9E-05
	Case 6		
	Volume [m3]	Volume fraction solid	β_0 [m/s]
Compartment 1	0,000020	0,30	0
Compartment 2	0,00032	0,56	8,1E-06
Compartment 3	0,00069	0,23	3,5E-06
Compartment 4	0,00019	0,17	5,8E-06
Compartment 5	0,00028	0,03	6,1E-07
Compartment 6	3,4E-05	0,48	3,6E-05
Compartment 7	4,7E-05	0,14	7,6E-06

Table 3. Flow rates to and from compartments for all cases.

Flow rates case 1 [m3/s]

0	1	2
1	0	0,007513
2	0,007513	0

Flow rates case 2 [m3/s]

0	1	2
1	0	0,007513
2	0,007513	0

Flow rates case 3 [m3/s]

	1	2	3
1	0	0,007513	0
2	0,007513	0	0,000948
3	0	0,00071	0

Flow rates case 4 [m3/s]

	1	2	3	4
1	0	0,007513	0	0
2	0,007513	0	0,000634	0,000392
3	0	0,00056	0	0
4	0	7,8E-05	0,0021	0

Flow rates case 5 [m3/s]

	1	2	3	4	5
1	0	0,0075	0	0	0
2	0,007513	0	0,000289	7,42E-08	0,000392
3	0	0,00019	0	0	0
4	0	0,00032	0,000672	0	0
5	0	7,8E-05	0	0,0021	0

Flow rates case 6 [m3/s]

	1	2	3	4	5	6	7
1	0	0,0075	0	0	0	0	0
2	0,007513	0	0,000643	0,000311	0	0,000327	0
3	0	0,00070	0	0	0,000318	0	5,3E-05
4	0	0,00047	0	0	0,000678	0	0
5	0	0	6,79E-05	0,000719	0	0	0
6	0	3,0E-05	0	0,0017	0	0	0,0015
7	0	0	4,9E-05	0	0,00010	0,0015	0